

ПАРАМЕТРЫ ПОДВОДНОГО РАЗРЯДА ПЕРЕМЕННОГО ТОКА

И.И. Ощенко, С.А. Смирнов

Иван Иванович Ощенко (ORCID 0000-0002-3949-8219), Сергей Александрович Смирнов* (ORCID 0000-0002-0375-0494)

Кафедра технологии приборов и материалов электронной техники, Ивановский государственный химико-технологический университет, Шереметевский пр., 7, Иваново, Российская Федерация, 153000
E-mail: sas@isuct.ru*, oshenko.ivan@yandex.ru

В работе приводятся результаты экспериментальных исследований параметров подводного разряда переменного тока частотой 50 Гц, горящего между двумя проволочными электродами из меди, молибдена и стали (Ст3). При различном межэлектродном расстоянии определены геометрические размеры пузырьков с микроразрядом (диаметр $0,54 \pm 0,03$ мм), вольтамперные характеристики разряда по которым оценены: длительность отдельных микроразрядов $\sim 1,0 \pm 0,2$ мс, падение напряжения между электродами 510 ± 60 В и приблизительная мощность тепловых источников нагрева жидкой фазы $\sim 120 \pm 10$ Вт. В зарегистрированных спектрах излучения разряда обнаружены линии атомарного водорода ($H_{\alpha}, H_{\beta}, H_{\gamma}$) и кислорода, а также полосы гидроксил радикала (переход $A^2\Sigma, V' \rightarrow X^2P, V'$). Полосы излучения молекулярного азота в спектре не обнаружены. Рассчитана абсолютная интенсивность излучения линий атомарного водорода и кислорода, а также полос гидроксил радикалов. В пределах погрешности измерения интенсивность излучения не зависит от материала электродов, но существенно изменяется с межэлектродным расстоянием. Рассчитана эффективная колебательная температура 7500 ± 300 К для $OH(A^2\Sigma)$. Заселенность вращательных уровней $OH(A^2\Sigma)$ можно описать двумя температурами, характеризующими нижние и верхние вращательные уровни с температурами 1800 ± 100 К и 3300 ± 200 К соответственно. Оцененная приведенная напряженность поля в исследованном разряде ($1,8 \pm 0,5 \cdot 10^{-16}$ В·см 2) в пределах погрешности определения не отличается от приведенной напряженности электрического поля положительного столба разряда атмосферного давления постоянного тока, горящего между металлическим электродом и водой. После зажигания разряда зарегистрировано изменение проводимости и pH жидкой фазы, выпадение микрокристаллического осадка оксидов металлов материала электродов.

Ключевые слова: неравновесный разряд, эмиссионная спектроскопия, напряженность поля, эффективная колебательная температура, температура газа, интенсивность излучения, плотность мощности источников нагрева

ALTERNATING CURRENT UNDERWATER DISCHARGE PARAMETERS

I.I. Oshchenko, S.A. Smirnov

Ivan I. Oshchenko ((ORCID 0000-0002-3949-8219), Sergey A. Smirnov* (ORCID 0000-0002-0375-0494)

Department of Electronic Devices and Materials, Ivanovo State University of Chemistry and Technology, Sheremetevskiy ave., 7, Ivanovo, 153000, Russia
E-mail: sas@isuct.ru*, oshenko.ivan@yandex.ru

The paper presents the results of experimental studies of the parameters of an underwater discharge of alternating current with a frequency of 50 Hz, burning between two wire electrodes made of copper, molybdenum and steel. At different interelectrode distances, the geometrical dimensions of bubbles with a microdischarge were determined, according to which the current-voltage characteristics of the discharge were estimated: the duration of individual microdischarges is $\sim 1.0 \pm 0.2$ ms, the voltage drop between the electrodes is 510 ± 60 V and the electric field strength is 510 ± 60 V/cm, the approximate power thermal sources of liquid phase heating $\sim 120 \pm 10$ W. In the recorded emission spectra of the discharge, lines of atomic hydrogen and oxygen, as well as bands of the hydroxyl radical, were found. There are no emission bands of molecular nitrogen in the spectrum. The absolute emission intensity of the lines of atomic hydrogen and oxygen, as well as the bands of hydroxyl radicals, has been calculated. Within the measurement error, the radiation intensity does not depend on the material of the electrodes, but varies significantly with the interelectrode distance. The effective vibrational temperature of 7500 ± 300 K for OH($A^2\Sigma$) is calculated. The population of rotational levels OH($A^2\Sigma$) can be described by two temperatures characterizing the lower and upper rotational levels with temperatures of 1800 ± 100 K and 3300 ± 200 K, respectively. The reduced electric field strength was estimated ($1.8 \cdot 10^{-16}$ V·cm 2). After the discharge was ignited, a change in the conductivity and pH of the liquid phase was registered, as well as the precipitation of a microcrystalline precipitate of metal oxides of the electrode material.

Key words: non-equilibrium discharge, emission spectroscopy, field strength, effective vibrational temperature, gas temperature, radiation intensity, power density of heating sources

Для цитирования:

Ощенко И.И., Смирнов С.А. Параметры подводного разряда переменного тока. *Изв. вузов. Химия и хим. технология.* 2022. Т. 65. Вып. 11. С. 6–12. DOI: 10.6060/ivkkt.20226511.6696.

For citation:

Oshchenko I.I., Smirnov S.A. Alternating current underwater discharge parameters. *ChemChemTech [Izv. Vyssh. Uchebn. Zaved. Khim. Khim. Tekhnol.]*. 2022. V. 65. N 11. P. 6–12. DOI: 10.6060/ivkkt.20226511.6696.

INTRODUCTION

Nonequilibrium plasma burning at atmospheric pressure is an effective tool in many areas of science, technology, biomedicine, and chemical technology [1–4]. The impact of atmospheric pressure plasma on the liquid phase opens up even greater opportunities for practical applications in analytical chemistry, water purification and disinfection, material processing, and chemical synthesis [6–10]. When a discharge is ignited in the liquid phase, various, both conductive and non-conductive liquids (for example, liquid nitrogen, ethanol, or deionized water) can be used as electrolytes. In this case, both the electrode and the ions of the solution can act as a source of particles. When an electrode is used as a starting material for nanoparticles, this is called “solution plasma sputtering” [11]. At present, it is not completely clear how breakdowns are formed in a liquid medium. The details of the breakdown process depend on the stresses and characteristics of the excitation wave, as well as on the properties of the liquid. However, DC or AC excitation can lead to Joule heating and the formation of a vapor phase through which breakdown can occur. It is believed that liquid discharges generated by microsecond pulses are initiated due to gas bubbles already present

in the liquid or bubbles formed when a voltage is applied. In this case, the formation of a discharge is also possible without bubbles [12], since nanosecond discharges are too short for bubbles to form during a high-voltage pulse.

To date, there is no single comprehensive theory describing the electrical breakdown of a liquid. It is natural to expect that the accumulation of experimental information about the discharge parameters in the liquid phase will make it possible to better understand the physics of this process.

The purpose of this work was to experimentally evaluate the electrophysical parameters of an underwater discharge using a variable power source with a frequency of 50 Hz and metal electrodes made of various materials.

EXPERIMENTAL TECHNIQUE

The discharge under study was excited in a quartz cell filled with distilled water (volume 50 ml) between two identical wire electrodes made of molybdenum, copper, and steel (St3sp) 1 mm in diameter [13]. The electrodes were located at an angle of 45° with respect to each other with the possibility of adjusting the interelectrode distance (L) 0.1–5 mm.

The discharge power circuit included a step-up transformer (maximum output voltage 10 kV), an adjustable laboratory autotransformer, and a ballast resistance of 6 k Ω . To determine the current-voltage characteristics of the discharge, a GWinstek GDS-71022 oscilloscope was used. In rare cases, with the configuration of the electrodes used and the set parameters (interelectrode distance, frequency and voltage amplitude), there is a possibility of a change in the type of discharge and the transition of a spark discharge to an arc discharge. Conductivity of the liquid phase and pH measurements was performed using PHT-028 (Kelinglong, China).

Plasma emission spectra were recorded using an AvaSpec-2048L-2-USB2 spectrophotometer with two 600 lines/mm diffraction gratings, operating wavelength range from 200 to 900 nm, and an entrance slit of $25 \times 100 \mu\text{m}$. The distance between the discharge burning site and the receiving lens of the spectrophotometer was 1.1 cm. Absolut emission intensity calculated $I = \hat{I}S_{Sl} \left(\frac{R_L^2}{4L_D^2} \pi R_D^2 H \right)^{-1}$, where \hat{I} – radiation intensity reduced to unit area of the entrance slit of the spectrometer, S_{Sl} – spectrophotometer slit area, R_L – radius receiving lens of the spectrophotometer 0.25 cm, L_D – distance from discharge to receiving lens of the spectrophotometer, H – discharge length, R_D – discharge radius.

To determine the rotational and vibrational temperatures OH(A $^2\Sigma$), we used the Cyber Wit Diatomic program or our own program [14]. Molecular constants for OH $^-$ were taken from the monograph [15]. It should be noted that in some cases it is impossible to describe the distribution of molecules over rotational levels by a single temperature. The reasons for this are detailed in the book by V.N. Ochkin [15]. The temperature of the arc discharge was determined by analyzing the slope of the continuum in the recorded radiation spectra [16]. The arc temperature did not depend on the material of the electrodes and the interelectrode distance and amounted to 5800 ± 500 K.

The determination of the approximate power density of heat sources for heating the liquid phase was carried out by analyzing the dependence of its temperature on time. The measurements were carried out with a pre-calibrated copper-constantan thermocouple in a thin-walled glass capillary at the heating section ($dT/dt)_H$ and the cooling section ($dT/dt)_C$ of the liquid phase (Fig. 1).

The power density of heat sinks and sources was calculated using the formula $cm(dT/dt) = \Sigma P_H - \Sigma P_C$. In this case, ΣP_H is the total power of all heat sources heating the system (time range from point 3 to point 4, Fig. 1),

and ΣP_C is the power of heat sinks in the system (time range from point 6, Fig. 1). According to experimental data for $L=5$ mm and $i=100$ mA $\Sigma P_H \approx 123$ W, and $\Sigma P_C \approx 18.1$ W.

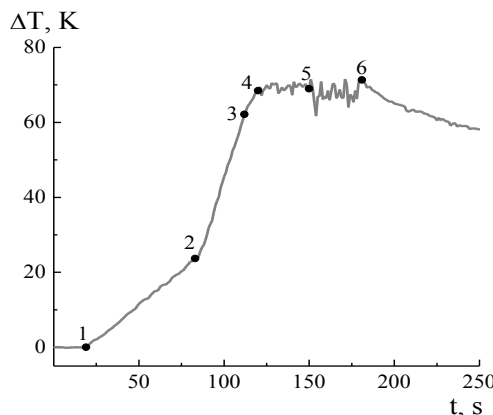


Fig. 1. Evolution temperature of liquid phase (Cu; L = 6.5 mm). 1 – the moment of switching on the power source of the system, the beginning of current transmission and generation of charge carriers ($i = 50$ mA); 2 – the end of the generation of charge carriers (t_1) and an increase in the current strength to the operating value (for example, $i = 100$ mA); 3 – moment of first spark (t_2); 4 – the beginning of the boiling of the liquid phase; 5 – the moment of achieving stable burning of the discharge; 6 – moment of switching off the power supply (t_3)

Рис. 1. Изменение температуры жидкой фазы внутри ячейки от времени (médные электроды; L = 6,5 mm). 1 – момент включения источника питания системы, начало пропускания тока и генерации носителей заряда ($i = 50$ mA); 2 – окончание генерации носителей заряда (t_1) и повышение силы тока до рабочего значения (например, $i = 100$ mA); 3 – момент первой искры (t_2); 4 – начало кипения жидкой фазы; 5 – момент достижения устойчивого горения разряда; 6 – момент выключения источника питания (t_3)

RESULTS AND DISCUSSION

The results of evaluating the conductivity and the value of the hydrogen index of the liquid phase are presented in Table 1. For all the experiments, the first 60 s of the installation operation was the “interval of charge carrier production” (t_G) during this time interval, the plasma discharge was not initiated, and the discharge current was maintained at the level 50 mA. Next, the operating value of the current (i) was set to 100 mA. Fig. 2 shows that the pH value has a non-linear dependence on the discharge generation time.

In the emission spectra of the discharge, emission lines of atomic hydrogen and oxygen, as well as bands of hydroxyl radicals (A $^2\Sigma$, V' \rightarrow X $^2\Pi$, V''), were recorded. In the emission spectra of a gas discharge burning between copper electrodes, numerous emission lines of copper are recorded. Similarly, the lines of atomic iron and molybdenum are present in the emission spectra of a discharge burning between steel

and molybdenum electrodes, respectively. No lines or bands of nitrogen-containing products were found in the emission spectra. It should be noted that the inter-

electrode distance has a noticeable effect on the emission intensities of the lines and bands of the spectrum (Fig. 3).

Table I
Characteristics of the liquid phase
Таблица 1. Характеристики жидкой фазы

Parameters	Electrode Cu–Cu			Electrode Fe–Fe			Electrode Mo–Mo			
	L, mm	t ₁	t ₂	t ₃	t ₁	t ₂	t ₃	t ₁	t ₂	t ₃
t, s	0.80	60	97	132	60	90	120	60	95	130
σ, 10 ⁻⁶ Sm		0.02	0.01	0.01	0.01	0.02	0.01	0.01	0.02	0.01
pH		5.46	5.81	6.16	5.56	6.00	6.26	5.60	5.81	6.06
t, s	1.40	60	117	143	60	95	130	60	99	141
σ, 10 ⁻⁶ Sm		0.01	0.02	0.02	0.02	0.03	0.03	0.04	0.05	0.03
pH		5.96	7.25	5.95	5.91	6.96	6.69	5.69	6.36	6.98
t, s	3.00	60	286	320	60	237	249	60	89	175
σ, 10 ⁻⁶ Sm		0.01	0.02	0.02	0.06	0.05	0.04	0.06	0.06	0.03
pH		6.11	8.45	6.55	6.11	8.39	7.03	5.46	6.10	5.63

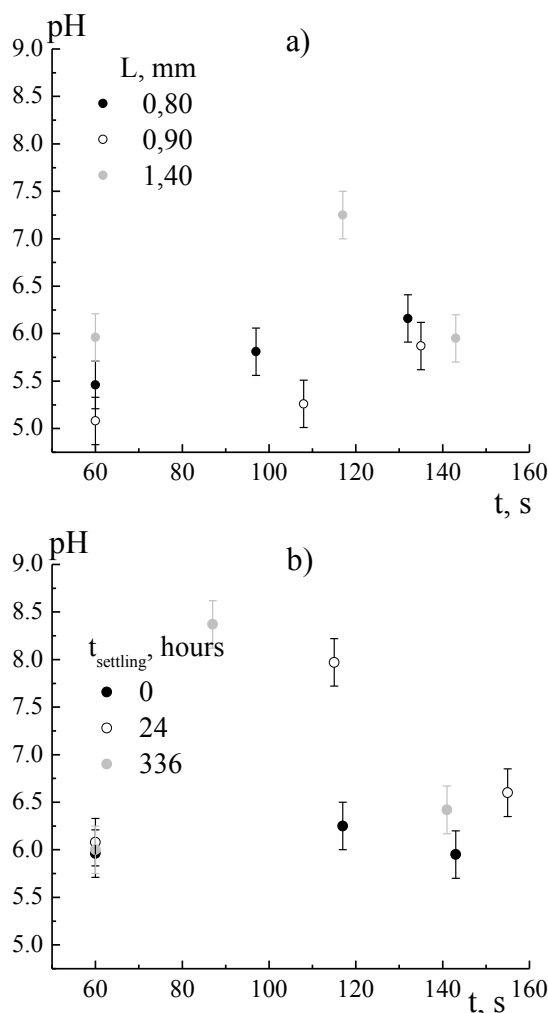


Fig. 2. Hydrogen index of the liquid phase after discharge burning at different interelectrode distances (a) and different settling times (b) (electrode Cu; i = 100 mA)

Рис. 2. Водородный показатель при различных межэлектродных расстояниях (а) и различном времени отстаивания (б) (медные электроды; i = 100 mA)

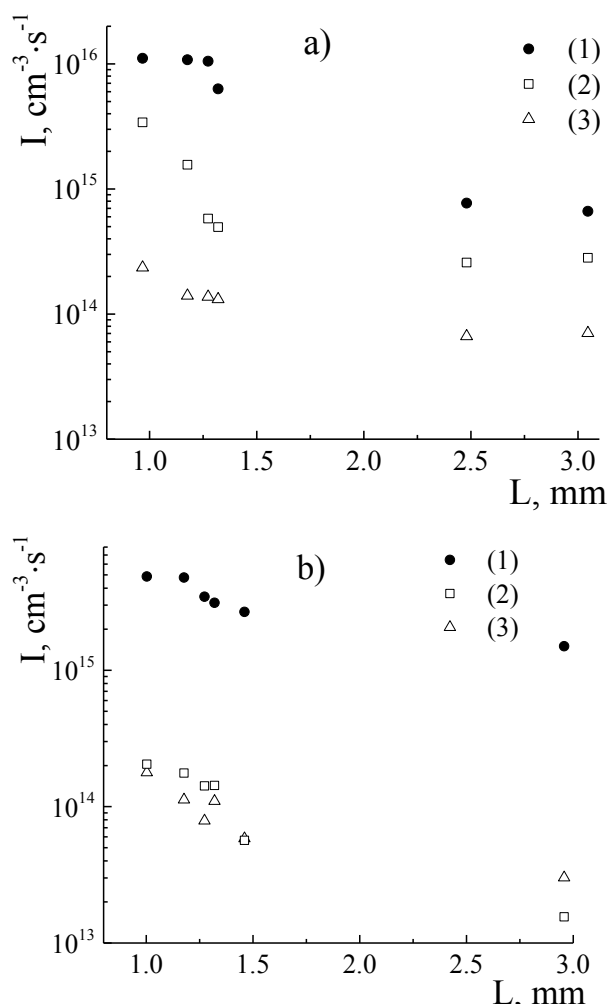


Fig. 3. The emission intensity of hydrogen lines for a burning discharge between copper (a) and steel (b) electrodes, 1 – H($2p^2P^0 \rightarrow 3d^2D$), 2 – H($2p^2P^0 \rightarrow 4d^2D$), 3 – H($2p^2P^0 \rightarrow 5d^2D$)

Рис. 3. Интенсивность излучения линий водорода для разряда горящего между медными (а) и стальными (б) электродами, 1 – H($2p^2P^0 \rightarrow 3d^2D$), 2 – H($2p^2P^0 \rightarrow 4d^2D$), 3 – H($2p^2P^0 \rightarrow 5d^2D$)

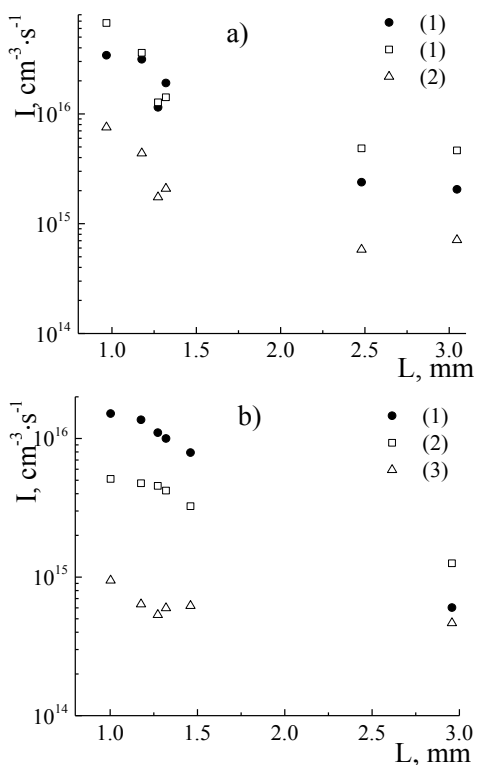


Fig. 4. The emission intensity of oxygen lines for a burning discharge between copper (a) and steel (b) electrodes,

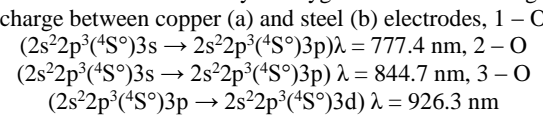


Рис. 4. Интенсивность излучения линий кислорода для разряда горящего между медными (а) и стальными (б) электродами 1 – O $(2s^22p^3(^4S^o))3s \rightarrow 2s^22p^3(^4S^o)3p \lambda = 777,4 \text{ нм}$, 2 – O $(2s^22p^3(^4S^o))3s \rightarrow 2s^22p^3(^4S^o)3p \lambda = 844,7 \text{ нм}$, 3 – O $(2s^22p^3(^4S^o))3p \rightarrow 2s^22p^3(^4S^o)3d \lambda = 926,3 \text{ нм}$

The effective vibrational temperature (T_v) and rotational temperature (T_r) of the $A^2\Sigma$ state were determined from the intensity ratio of the OH bands at different interelectrode distances (Table 2). It should be noted that there are two groups of cold and hot molecules corresponding to the lower and higher rotational numbers of the $A^2\Sigma$ state with temperatures of $1800 \pm 100 \text{ K}$ (we equated the gas temperature) and $3300 \pm 200 \text{ K}$, respectively.

The digital photograph was used to determine the geometrical parameters of the discharge channel. Despite the fact that the observed plasma is actually a

group of successive microdischarges, in the interval of several seconds one can speak of the existence of a stable path along which the bulk of the discharges pass. The initially formed area of the discharge burning is shifted to the surface of the liquid phase, which leads to an elongation of the discharge channel and subsequently to its rupture. In most cases, we can say that the length of the discharge channel is greater than the interelectrode distance by $\sim 20\text{-}30\%$ for all types of electrodes we studied.

The frequency of initiation of single discharges in the vast majority of cases coincides with the frequency of the current. Under the same conditions, individual microdischarges are almost completely identical, but are accompanied by stochastic current fluctuations. The duration of a single discharge, which was 1.2 ± 0.3 milliseconds. The microdischarge voltage is practically independent of time and amounts to $\sim 560 \pm 40 \text{ V}$ (Fig. 5). The microdischarge current, without taking into account random fluctuations, reaches $273 \pm 35 \text{ mA}$ (Fig. 5).

The estimated reduced field strength in the discharge we studied (Table 2) within the limits of the determination error does not differ from the reduced electric field strength of the positive column of the DC atmospheric pressure discharge burning between the metal electrode and water [17-20].

CONCLUSION

The results of the study of the parameters of an electric discharge in the liquid phase when using an alternating power source with a frequency of 50 Hz are presented. The digital photos, radiation spectra and volt-ampere characteristics of the discharge were recorded, the thermal sources of heating of the liquid phase and the geometric parameters of the discharge were evaluated.

The study was carried out using the resources of the Center for Shared Use of Scientific Equipment of the ISUCT (with the support of the Ministry of Science and Higher Education of Russia, grant No. 075-15-2021-671).

Исследование выполнено с использованием ресурсов Центра коллективного пользования научной аппаратурой ИГХТУ (при поддержке Минобрнауки России, грант № 075-15-2021-671).

Table 2

Plasma electro physical parameters
Таблица 2. Электрофизические параметры

Electrodes	$T_r, \text{ K}$	$i, \text{ A}$	$E, \text{ V/cm}$	$N, \text{ cm}^{-3}$	$E/N, \text{ V}\cdot\text{cm}^2$	$D, \text{ cm}$	$T_v, \text{ K}$	$\tau, \text{ ms}$
Mo– Mo	1700	0.276	513	$2.94 \cdot 10^{18}$	$1.75 \cdot 10^{-16}$	0.054	7500	1.34
Cu– Cu	1800	0.256	448	$2.45 \cdot 10^{18}$	$1.83 \cdot 10^{-16}$	0.057	7600	0.96
Fe– Fe	1600	0.321	569	$2.62 \cdot 10^{18}$	$2.17 \cdot 10^{-16}$	0.052	7700	0.79

Note: ^ainterelectrode distance 3 mm

Примечание: ^aрасстояние между электродами 3 мм

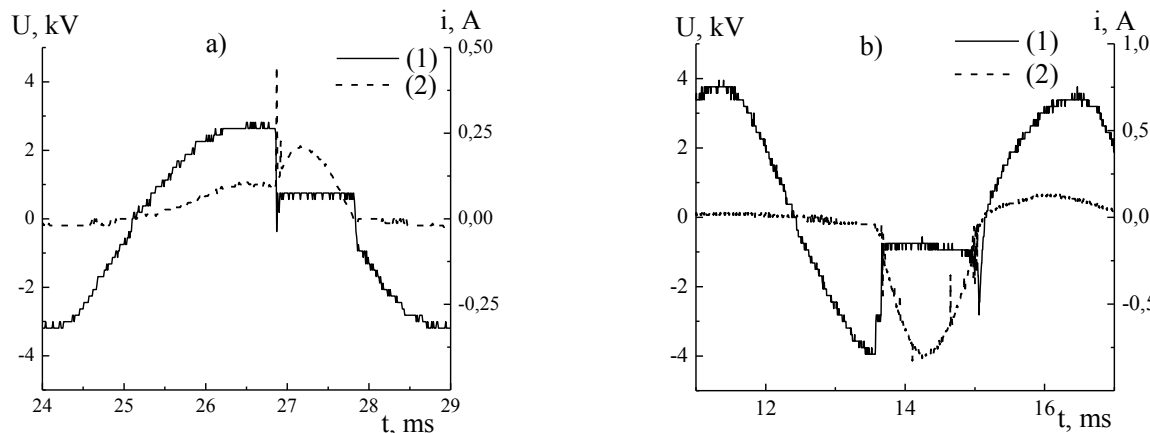


Fig. 5. Voltage (1) and current (2) change at the discharge between two electrodes made of copper (a) and molybdenum (b); interelectrode distance is 3 mm

Рис. 5. Изменения напряжения (1) и тока (2) микроразряда горящего между медными (а) и молибденовыми (б) электродами; межэлектродное расстояние 3 мм

Авторы заявляют об отсутствии конфликта интересов, требующего раскрытия в данной статье.

The authors declare the absence a conflict of interest warranting disclosure in this article.

ЛИТЕРАТУРА

- Акишев Ю.С. Низкотемпературная плазма при атмосферном давлении и ее возможности для приложений. *Изв. вузов. Химия и хим. технология*. 2019. Т. 62. Вып. 8. С. 26-60. DOI: 10.6060/ivkkt.20196208.5908.
- Becker K.H., Kogelschatz U., Schoenbach K.H., Barker R.J. Non-equilibrium air plasmas at atmospheric pressure. Institute of Physics Publ. 2005. 682 p. DOI: 10.1201/9781482269123.
- Fridman A., Kennedy L.A. Plasma Physics and Engineering. New York, London: Taylor & Francis. 2004. 853 p. DOI: 10.1201/9781315120812.
- Гордина Н.Е., Мельников А.А., Гусев Г.И., Гущин А.А., Румянцев Р.Н., Астраханцева И.А. Использование механохимической и плазмохимической обработок при синтезе каталитических систем на основе вермикулита и оксихлорида циркония. *Изв. вузов. Химия и хим. технология*. 2022. Т. 65. Вып. 5. С. 43-57. DOI: 10.6060/ivkkt.20226505.6612.
- Гусев Г.И., Гущин А.А., Гриневич В.И., Извекова Т.В., Квиткова Е.Ю., Рыбкин В.В. Деструкция водных растворов 2,4-дихлорфенола в плазменно-катализитическом реакторе барьерного разряда. *Изв. вузов. Химия и хим. технология*. 2021. Т. 64. Вып. 11. С. 103-111. DOI: 10.6060/ivkkt.20216411.6507.
- Манукян А.С., Сейоум М.Б., Рыбкин В.В. Разложение органических красителей в их водных растворах под действием электрических разрядов атмосферного давления. *Изв. вузов. Химия и хим. технология*. 2021. Т. 64. Вып. 3. С. 4-12. DOI: 10.6060/ivkkt.20216403.6339.
- Смирнова К.В., Шутов Д.А., Иванов А.Н., Манукян А.С., Рыбкин В.В. Плазма-растворный синтез оксида железа (III). *Изв. вузов. Химия и хим. технология*. 2021. Т. 64. Вып. 7. С. 83-88. DOI: 10.6060/ivkkt.20216407.6409.
- Шутов Д.А., Сунгуррова А.В., Смирнова К.В., Манукян А.С., Рыбкин В.В. Оксидительно-восстановительные процессы с участием ионов марганца, инициируемые тлеющим разрядом, в водном растворе. *Изв. вузов. Химия и*

REFERENCES

- Akishev Yu.S. Non-thermal plasma at atmospheric pressure and its opportunities for applications. *ChemChemTech [Izv. Vyssh. Uchebn. Zaved. Khim. Khim. Tekhnol.]*. 2019. V. 62. N 8. P. 26-60 (in Russian). DOI: 10.6060/ivkkt.20196208.5908.
- Becker K.H., Kogelschatz U., Schoenbach K.H., Barker R.J. Non-equilibrium air plasmas at atmospheric pressure. Institute of Physics Publ. 2005. 682 p. DOI: 10.1201/9781482269123.
- Fridman A., Kennedy L.A. Plasma Physics and Engineering. New York, London: Taylor & Francis. 2004. 853 p. DOI: 10.1201/9781315120812.
- Gordina N.E., Melnikov A.A., Gusev G.I., Gushchin A.A., Rumyantsev R.N., Astrakhantseva I.A. The use of mechanochemical and plasma-chemical treatments in the synthesis of catalytic systems based on vermiculite and zirconium oxychloride. *ChemChemTech [Izv. Vyssh. Uchebn. Zaved. Khim. Khim. Tekhnol.]*. 2022. V. 65. N 5. P. 43-57 (in Russian). DOI: 10.6060/ivkkt.20226505.6612.
- Gusev G.I., Gushchin A.A., Grinevich V.I., Izvekova T.V., Kvitkova E.Yu., Rybkin V.V. Destruction of Aqueous Solutions of 2,4-Dichlorophenol in a Plasma Catalytic Barrier Discharge Reactor. *ChemChemTech [Izv. Vyssh. Uchebn. Zaved. Khim. Khim. Tekhnol.]*. 2021. V. 64. N 11. P. 103-111 (in Russian). DOI: 10.6060/ivkkt.20216411.6507.
- Manukyan A.S., Seyoum M.B., Rybkin V.V. Decomposition of organic dyes in their aqueous solutions under action of electric discharges of atmospheric pressure. *ChemChemTech [Izv. Vyssh. Uchebn. Zaved. Khim. Khim. Tekhnol.]*. 2021. V. 64. N 3. P. 4-12. DOI: 10.6060/ivkkt.20216403.6339.
- Smirnova K.V., Shutov D.A., Ivanov A.N., Manukyan A.S., Rybkin V.V. Plasma-solution synthesis of iron (III) oxide. *ChemChemTech [Izv. Vyssh. Uchebn. Zaved. Khim. Khim. Tekhnol.]*. 2021. V. 64. N 7. P. 83-88. DOI: 10.6060/ivkkt.20216407.6409.
- Shutov D.A., Sungurova A.V., Smirnova K.V., Manukyan A.S., Rybkin V.V. Oxidative-reducing processes with participation of manganese ions initiated by electric discharge in aqueous solution. *ChemChemTech [Izv. Vyssh. Uchebn. Zaved. Khim. Khim. Tekhnol.]*. 2018. V. 61. N 9. P. 23-29. DOI: 10.6060/ivkkt.20186109-10.5802.

- хим. технология. 2018. Т. 61. Вып. 9-10. С. 23-29. DOI: 10.6060/ivkkt20186109-10.5802.
9. Гусев Г.И., Гущин А.А., Гриневич В.И., Рыбкин В.В., Извекова Т.В., Шаронов А.В. Обработка сточных вод, содержащих 2,4-дихлорофенол, в плазме диэлектрического барьера разряда. *Изв. вузов. Химия и хим. технология.* 2020. Т. 63. Вып. 7. С. 88-94. DOI: 10.6060/ivkkt.20206307.6182.
10. Шутов Д.А., Иванов А.Н., Рыбкин В.В., Манукян А.С. Сравнительное изучение электрофизических характеристик тлеющего разряда надводными растворами анион активных и катион активных поверхностно-активных веществ. *Изв. вузов. Химия и хим. технология.* 2020. Т. 63. Вып. 2. С. 91-98. DOI: 10.6060/ivkkt.20206302.6194.
11. Hu X., Shen X., Takai O., Saito N. Facile fabrication of PtAu alloy clusters using solution plasma sputtering and their electrocatalytic activity. *J. Alloys Compd.* 2013. V. 552. P. 351-355. DOI: 10.1016/J.JALLCOM.2012.08.033.
12. Starikovskiy A., Yang Y., Cho Y. Non-equilibrium plasma in liquid water: dynamics of generation and quenching. *Plasma Sour. Sci. Technol.* 2011. N 2. P. 1-7. DOI: 10.1088/0963-0252/20/2/024003.
13. Oshenko I.I., Smirnov S.A. Electrophysical parameters of AC plasma system. *J. Phys.: Conf. Ser.* 2022. 2270. P. 012027. DOI: 10.1088/1742-6596/2270/1/012027.
14. CyberWit Diatomic http://cyber-wit.com/products_Diatomic.html
15. Ochkin V.N. Spectroscopy of Low Temperature Plasma. Wiley-VCH. 2009. 630 p. DOI: 10.1002/9783527627509.
16. Лапшинов Б.А., Суворинов А.В., Тимченко Н. Определение температуры излучающего объекта методом спектральной пирометрии. *Контроль Измерения.* 2018. Вып. 6. С. 116-119. DOI: 10.22184/1992-4178.2018.177.6.116.119.
17. Коновалов А.С., Голубев С.Н., Иванов А.Н., Шутов Д.А., Смирнов С.А., Рыбкин В.В. Электрофизические параметры тлеющего разряда с жидким электродом в атмосфере воздуха при пониженном давлении. *Изв. вузов. Химия и хим. технология.* 2012. Т. 55. Вып. 12. С. 55-58.
18. Bobkova E.S., Smirnov S.A., Zalipaeva Ya.V., Rybkin V.V. Modeling Chemical Composition for an Atmospheric Pressure DC Discharge in Air with Water Cathode by 0-D model. *Plasma Chem. and Plasma Proc.* 2014. V. 34. N 4. P. 721 – 743. DOI: 10.1007/s11090-014-9539-z.
19. Петров А.Е., Титов В.А., Смирнов С.А. Концентрация атомов кислорода в тлеющем разряде атмосферного давления в воздухе. *Изв. вузов. Химия и хим. технология.* 2013. Т. 56. Вып. 2. С. 80-84.
20. Titov V.A., Rybkin V.V., Smirnov S.A., Kulentsan A.L., Ho-Suk Choi. Properties of atmospheric pressure glow discharge with liquid electrolyte cathode. *High Temp. Mater. Proc.* 2007. V. 11. N 4. P. 515 – 526. DOI: 10.1615/HighTempMatProc.v11.i4.40.
9. Gusev G.I., Gushchin A.A., Grinevich V.I., Rybkin V.V., Izvekova T.V., Sharonov A.V. Treatment of wastewater containing 2,4-dichlorophenol in dielectric barrier discharge plasma. *ChemChemTech [Izv. Vyssh. Uchebn. Zaved. Khim. Khim. Tekhnol.]*. 2020. V. 63. N 7. P. 88-94. DOI: 10.6060/ivkkt.20206307.6182.
10. Shutov D.A., Ivanov A.N., Rybkin V.V., Manukyan A.S. Comparative Study of the Electrophysical Characteristics of a Glow Discharge with Surface Solutions of Anion Active and Cation Active Surfactants. *ChemChemTech [Izv. Vyssh. Uchebn. Zaved. Khim. Khim. Tekhnol.]*. 2020. V. 63. N 2. P. 91-98. DOI: 10.6060/ivkkt.20206302.6194.
11. Hu X., Shen X., Takai O., Saito N. Facile fabrication of PtAu alloy clusters using solution plasma sputtering and their electrocatalytic activity. *J. Alloys Compd.* 2013. V. 552. P. 351-355. DOI: 10.1016/J.JALLCOM.2012.08.033.
12. Starikovskiy A., Yang Y., Cho Y. Non-equilibrium plasma in liquid water: dynamics of generation and quenching. *Plasma Sour. Sci. Technol.* 2011. N 2. P. 1-7. DOI: 10.1088/0963-0252/20/2/024003.
13. Oshenko I.I., Smirnov S.A. Electrophysical parameters of AC plasma system. *J. Phys.: Conf. Ser.* 2022. 2270. P. 012027. DOI: 10.1088/1742-6596/2270/1/012027.
14. CyberWit Diatomic http://cyber-wit.com/products_Diatomic.html
15. Ochkin V.N. Spectroscopy of Low Temperature Plasma. Wiley-VCH. 2009. 630 p. DOI: 10.1002/9783527627509.
16. Lapshinov B.A., Suvorinov A.V., Timchenko N. Determination of the temperature of the emitting object by spectral pyrometry. *Kontrol' Izmereniya.* 2018. N 6. P. 116-119 (in Russian). DOI: 10.22184/1992-4178.2018.177.6.116.119.
17. Konovalov A.S., Golubev S.N., Ivanov A.N., Shutov D.A., Smirnov S.A., Rybkin V.V. Electrophysical parameters of a glow discharge with a liquid electrode in air at reduced pressure. *ChemChemTech [Izv. Vyssh. Uchebn. Zaved. Khim. Khim. Tekhnol.]*. 2012. V. 55. N 12. P. 55-58 (in Russian).
18. Bobkova E.S., Smirnov S.A., Zalipaeva Ya.V., Rybkin V.V. Modeling Chemical Composition for an Atmospheric Pressure DC Discharge in Air with Water Cathode by 0-D model. *Plasma Chem. and Plasma Proc.* 2014. V. 34. N 4. P. 721 – 743. DOI: 10.1007/s11090-014-9539-z.
19. Petrov A.E., Titov V.A., Smirnov S.A. The concentration of oxygen atoms in a glow discharge of atmospheric pressure in air. *ChemChemTech [Izv. Vyssh. Uchebn. Zaved. Khim. Khim. Tekhnol.]*. 2013. V. 56. N 2. P. 80-84 (in Russian).
20. Titov V.A., Rybkin V.V., Smirnov S.A., Kulentsan A.L., Ho-Suk Choi. Properties of atmospheric pressure glow discharge with liquid electrolyte cathode. *High Temp. Mater. Proc.* 2007. V. 11. N 4. P. 515 – 526. DOI: 10.1615/HighTempMatProc.v11.i4.40.

Поступила в редакцию 29.06.2022
Принята к опубликованию 23.08.2022

Received 29.06.2022
Accepted 23.08.2022